

## Oxygen Environment of Rare-Earth Ions in Phosphates with $\beta$ -K<sub>2</sub>SO<sub>4</sub> Type Structure

MM. M. BEN AMARA, C. PARENT, M. VLASSE, AND G. LE FLEM

*Laboratoire de Chimie du Solide du CNRS, 351, cours de la Libération, 33405 Talence Cédex, France*

Received July 26, 1982; and in revised form September 18, 1982

The use of europium as a local structure probe allowed the authors to determine the various phases appearing at room temperature in the NaPO<sub>4</sub>-Na<sub>3</sub>Eu(PO<sub>4</sub>)<sub>2</sub> and NaSrPO<sub>4</sub>-Na<sub>3</sub>Eu(PO<sub>4</sub>)<sub>2</sub> systems. The broadening of the europium emission lines in going from the calcium to the strontium phases illustrates the ease of movement of the [PO<sub>4</sub>] groups.

Two structural features characterize the  $\beta$ -K<sub>2</sub>SO<sub>4</sub> type structure:

(1) a central [KO<sub>6</sub>] octahedron sharing corners with six tetrahedral [SO<sub>4</sub>] groups;

(2) Along the pseudo-three-fold axis of the octahedron, strings of potassium atoms and [SO<sub>4</sub>] units (*A*), alternating with strings of potassium atoms only (*B*) (1, 2).

At rising temperature the low temperature (L.T.)  $\beta$  form transforms into a high temperature (H.T.) hexagonal  $\alpha$  form. This transformation results from the alignment of the potassium along the B strings and a reorientation of the tetrahedra (3-5) (Fig. 1).

A great number of compounds are known to have a structure related to  $\beta$ -K<sub>2</sub>SO<sub>4</sub>-type, such as NaMPO<sub>4</sub> (*M* = Ca, Sr, Ba) or Na<sub>3</sub>Ln(PO<sub>4</sub>)<sub>2</sub> (*Ln* = rare earth). Most of them have a H.T. hexagonal form, which transforms into a L.T. one by appearance of a cationic ordering in the *B* sublattice and by rotation of the [XO<sub>4</sub>] groups around the common corners with the central octahedron. This rotation leads to the various anionic environments required by the *B* cations (6-8). In the Na<sub>3</sub>Ln(PO<sub>4</sub>)<sub>2</sub> L.T. phases

this rotational mobility of the [XO<sub>4</sub>] groups produces a variety of complex structures, in which the rare-earth ion may occupy several different crystallographic sites (9).

The analysis of the fluorescence spectra of Eu<sup>3+</sup> in Na<sub>3</sub>Eu(PO<sub>4</sub>)<sub>2</sub> has shown the existence of two low temperature varieties  $\delta$  and  $\epsilon$  having europium in 8 and 3 independent sites, respectively. However, their X-ray diffraction spectra showed no perceptible difference. In addition, in each of these phases, the position of the fluorescence lines <sup>5</sup>D<sub>0</sub> → <sup>7</sup>F<sub>0</sub> indicates that the europium sites have a quite similar anionic environment and the passage from one to other ( $\delta$  →  $\epsilon$ ) can result from a slight rotation of the [PO<sub>4</sub>] tetrahedra without changing in any way the cationic sublattice (10) (Fig. 2).

Therefore, it was worthwhile to consider materials in which the energy difference between the various [PO<sub>4</sub>] positions would be so small that, in terms of anionic environment, a continuum of crystallographic sites could exist for the *B* chain cations.

Such a situation was found in the low temperature phases of the systems Na

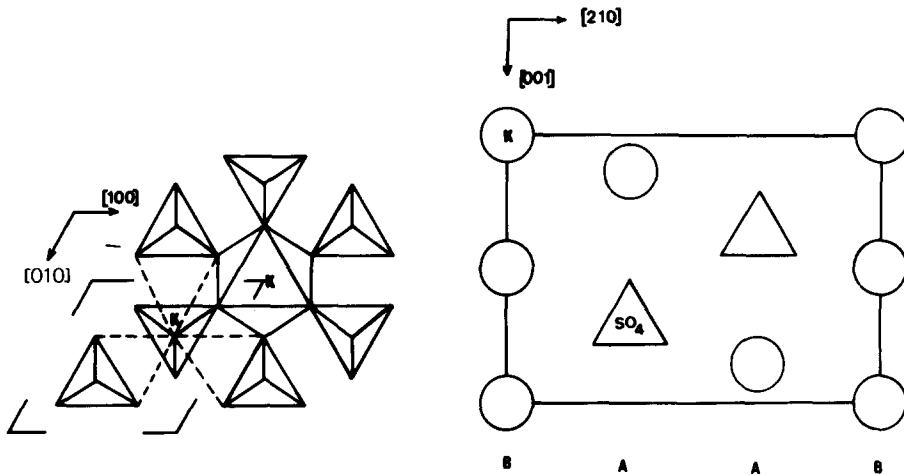


FIG. 1. Main features of the  $\alpha$ - $K_2SO_4$ -type structure.

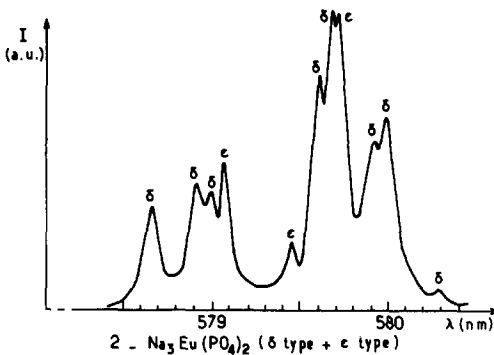
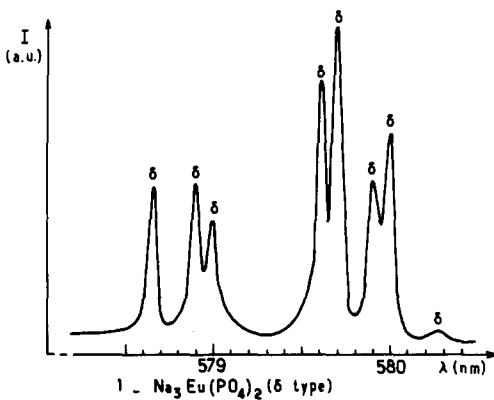


FIG. 2.  $^5D_0 \rightarrow ^7F_0$  emission of  $Eu^{3+}$  in  $Na_3Eu(PO_4)_2$  under 380 nm excitation ( $T = 80$  K): (1)  $\delta$ -type; (2)  $\delta$ -type +  $\epsilon$ -type.

$CaPO_4-Na_3Eu(PO_4)_2$  and  $NaSrPO_4-Na_3Eu(PO_4)_2$  by comparison of their structural and optical properties.

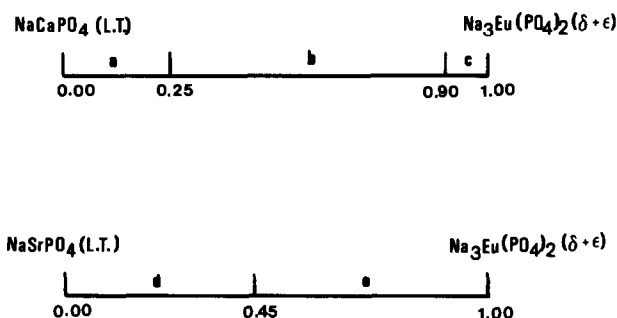
### Crystallographic Study of the $NaCaPO_4-Na_3Eu(PO_4)_2$ and $NaSrPO_4-Na_3Eu(PO_4)_2$ systems

Although the  $NaCaPO_4$  L.T. phase is known, its symmetry and lattice parameters are still much debated (6, 11, 12). Sin-

TABLE I

$^5D_0 \rightarrow ^7F_j$  ( $j = 0, 1, 2$ ) EMISSION OF  $Eu^{3+}$  IN  $Na_{2.20}Ca_{1.60}Eu_{0.20}(PO_4)_2$  ( $a$  TYPE) UNDER 380-nm EXCITATION ( $T = 80$  K)

$a$ Type	$T = 80$ K		
	$\lambda$ (nm)	$E$ ( $cm^{-1}$ )	
$Na_{2.20}Ca_{1.60}Eu_{0.20}(PO_4)_2$			
	$^5D_0 \rightarrow ^7F_0$	579.9	17,244
	$^5D_0 \rightarrow ^7F_1$	588.7	16,986
		593.3	16,855
594.8		16,812	
$^5D_0 \rightarrow ^7F_2$	611.9	16,342	
	613.7	16,295	
	615.7	16,242	
	619.6	16,139	
	622.4	16,067	


 FIG. 3. Composition ranges of the different structural types obtained with rising  $\text{Eu}^{3+}$  content.

gle crystals were prepared from a  $\text{Na}_2\text{MoO}_4$  flux. The orthorhombic lattice constants of the crystals are related to those of  $\beta\text{-K}_2\text{SO}_4$  in the following way:

$$a_{\text{NaCaPO}_4} \approx 3a_{\beta\text{-K}_2\text{SO}_4}$$

$$b_{\text{NaCaPO}_4} \approx b_{\beta\text{-K}_2\text{SO}_4}$$

$$c_{\text{NaCaPO}_4} \approx c_{\beta\text{-K}_2\text{SO}_4}$$

A more detailed structural determination is in progress.

Single crystals of  $\text{NaSrPO}_4$  were also grown in a  $\text{Na}_2\text{MoO}_4$  flux. They have a hexagonal symmetry with parameters  $a =$

$27.23 \text{ \AA}$ ,  $c = 36.36 \text{ \AA}$ . These large dimensions, confirmed by electron diffraction, make an X-ray structural study very difficult. However, the reciprocal lattice shows a hexagonal sublattice whose parameters,  $a_0 = a/5$ ,  $c_0 = c/5$ , are close to those of  $\alpha\text{-K}_2\text{SO}_4$ .

At low temperature the  $\text{NaCaPO}_4\text{-Na}_3\text{Eu}(\text{PO}_4)_2$  phase diagram shows three main regions.

The first domain (*a*) exists up to composition  $\text{Na}_{2.25}\text{Ca}_{1.50}\text{Eu}_{0.25}(\text{PO}_4)_2$  with the structure of  $\text{NaCaPO}_4$  (L.T.). The superstructure lines disappear already for samples with low europium content and then the spectrum can be indexed on the basis of the  $\beta\text{-K}_2\text{SO}_4$  type structure.

The second region (*b*) appears up to the composition  $\text{Na}_{2.90}\text{Ca}_{0.20}\text{Eu}_{0.90}(\text{PO}_4)_2$ . Its structure is that of  $\text{Na}_3\text{Nd}(\text{VO}_4)_2$  (L.T.), where the neodymium atoms occupy three different crystallographic sites (13).

TABLE II

$^5D_0 \rightarrow ^7F_j$  ( $j = 0, 1$ ) EMISSION OF  $\text{Eu}^{3+}$  IN  $\text{Na}_{2.80}\text{Ca}_{0.40}\text{Eu}_{0.80}(\text{PO}_4)_2$  (*b* TYPE) UNDER 380-nm EXCITATION ( $T = 80 \text{ K}$ )

<i>b</i> Type	$T = 80 \text{ K}$		
	$\lambda$ (nm)	$E$ ( $\text{cm}^{-1}$ )	
$\text{Na}_{2.80}\text{Ca}_{0.40}\text{Eu}_{0.80}(\text{PO}_4)_2$			
$^5D_0 \rightarrow ^7F_0$	579.4	17,259	
	579.7	17,250	
	580.0	17,241	
	$^5D_0 \rightarrow ^7F_1$	587.9	17,010
		588.3	16,998
		590.0	16,949
		592.0	16,892
		595.2	16,801
		596.2	16,773
		597.2	16,745
597.9	16,725		
599.9	16,669		

TABLE III

$^5D_0 \rightarrow ^7F_0$  EMISSION OF  $\text{Eu}^{3+}$  IN  $\text{Na}_{2.95}\text{Ca}_{0.10}\text{Eu}_{0.95}(\text{PO}_4)_2$  (*c* TYPE) UNDER 380-nm EXCITATION ( $T = 80 \text{ K}$ )

<i>c</i> Type	$T = 80 \text{ K}$	
	$\lambda$ (nm)	$E$ ( $\text{cm}^{-1}$ )
$\text{Na}_{2.95}\text{Ca}_{0.10}\text{Eu}_{0.95}(\text{PO}_4)_2$		
$^5D_0 \rightarrow ^7F_0$	579.1	17,268
	579.5	17,256
	579.8	17,250

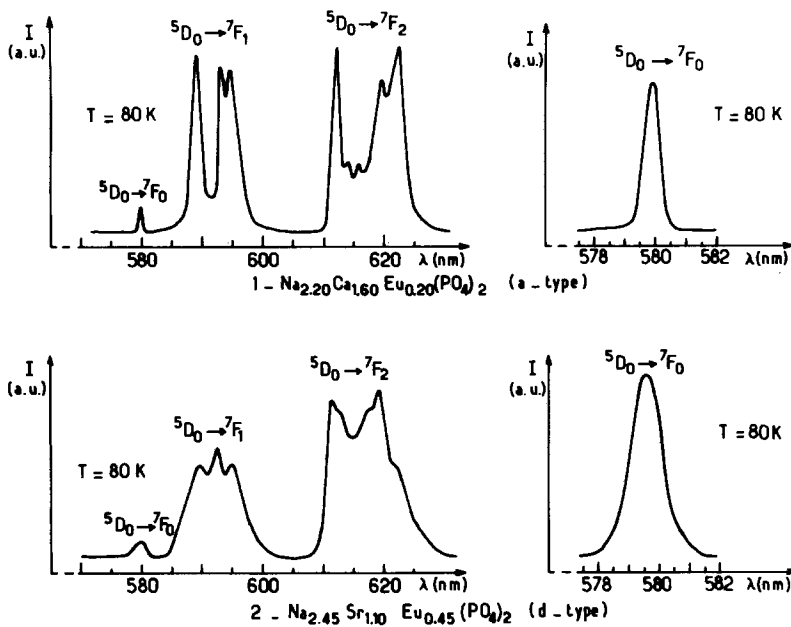


FIG. 4. Emission spectrum of  $\text{Eu}^{3+}$  under 380 nm excitation ( $T = 80 \text{ K}$ ) in (1)  $\text{Na}_{2.20}\text{Ca}_{1.60}\text{Eu}_{0.20}(\text{PO}_4)_2$  (a type); (2)  $\text{Na}_{2.45}\text{Sr}_{1.1}\text{Eu}_{0.45}(\text{PO}_4)_2$  (d type).

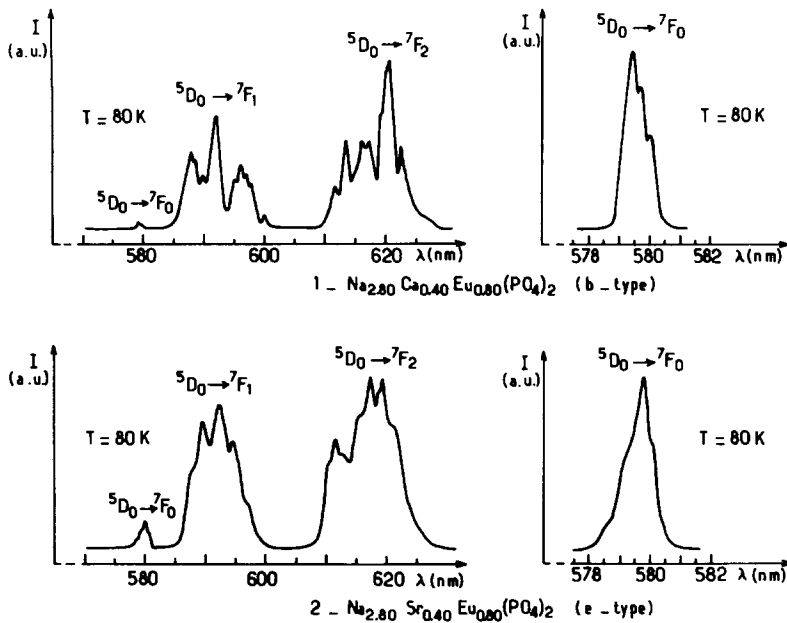


FIG. 5. Emission spectrum of  $\text{Eu}^{3+}$  under 380 nm excitation ( $T = 80 \text{ K}$ ) in (1)  $\text{Na}_{2.80}\text{Ca}_{0.40}\text{Eu}_{0.80}(\text{PO}_4)_2$  (b type); (2)  $\text{Na}_{2.80}\text{Sr}_{0.40}\text{Eu}_{0.80}(\text{PO}_4)_2$  (e type).

The upper limit of the third domain (*c*) corresponds to  $\text{Na}_3\text{Eu}(\text{PO}_4)_2$  composition. Its diffraction spectrum can be indexed with the  $\text{Na}_3\text{Eu}(\text{PO}_4)_2$ -type structure ( $\delta$  or  $\epsilon$ ).

The  $\text{NaSrPO}_4$ - $\text{Na}_3\text{Eu}(\text{PO}_4)_2$  phase diagram shows only two existence regions at low temperature. The first domain (*d*) with the  $\text{NaSrPO}_4$  (L.T.) structure exists up to composition  $\text{Na}_{2.45}\text{Sr}_{1.10}\text{Eu}_{0.45}(\text{PO}_4)_2$ .

A single crystal diffraction study of this material pointed out the positions of the heavy atoms but did not allow us to localize the  $[\text{PO}_4]$  positions.

The second domain (*e*) extends up to  $\text{Na}_3\text{Eu}(\text{PO}_4)_2$  and is isotypic with  $\text{Na}_3\text{Eu}(\text{PO}_4)_2$  ( $\delta$  or  $\epsilon$ ). Figure 3 summarizes these results.

### Optical Study of the $\text{NaCaPO}_4$ (L.T.)- $\text{Na}_3\text{Eu}(\text{PO}_4)_2$ ( $\delta+\epsilon$ ) and $\text{NaSrPO}_4$ (L.T.)- $\text{Na}_3\text{Eu}(\text{PO}_4)_2$ ( $\delta+\epsilon$ ) systems

The  ${}^5D_0 \rightarrow {}^7F_j$  ( $j = 0, 1, 2$ ) europium emission has been studied under 380 nm excitation at 80 K for compositions representing the five existence regions observed.

The spectrum of the phase with composition (*a* region)  $\text{Na}_{2.20}\text{Ca}_{1.60}\text{Eu}_{0.20}(\text{PO}_4)_2$  shows one, three and five lines for  $j = 0, 1, 2$ , respectively (Fig. 4-1). The europium atom occupies, therefore, only one type of noncentrosymmetric site and must be statistically distributed in the *B* chain sublattice. This fact confirms the isotropy of this phase with  $\beta$ - $\text{K}_2\text{SO}_4$ .

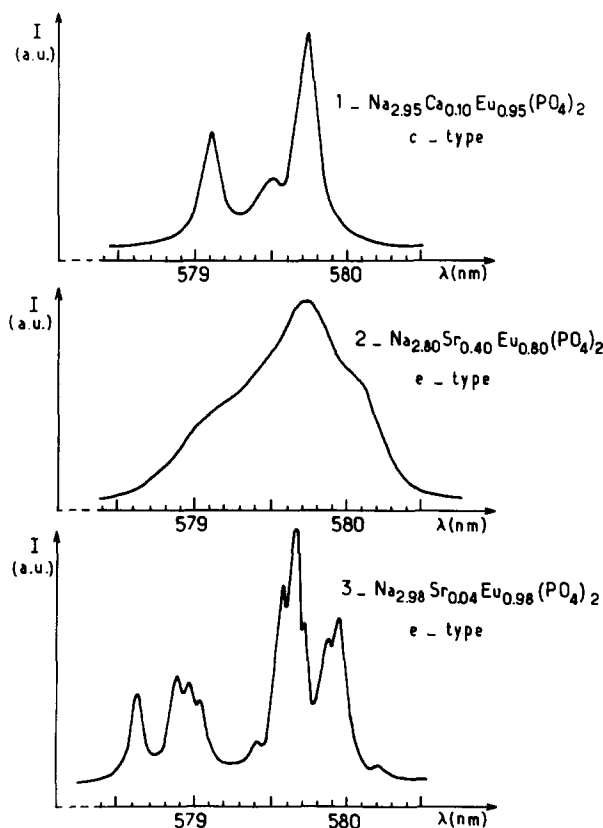


FIG. 6.  ${}^5D_0 \rightarrow {}^7F_0$  emission of  $\text{Eu}^{3+}$  under 380 nm excitation ( $T = 80$  K) in (1)  $\text{Na}_{2.95}\text{Ca}_{0.10}\text{Eu}_{0.95}(\text{PO}_4)_2$  (*c* type); (2)  $\text{Na}_{2.80}\text{Sr}_{0.40}\text{Eu}_{0.80}(\text{PO}_4)_2$  (*e* type); (3)  $\text{Na}_{2.98}\text{Sr}_{0.04}\text{Eu}_{0.98}(\text{PO}_4)_2$  (*e* type).

The spectrum of  $\text{Na}_{2.80}\text{Ca}_{0.40}\text{Eu}_{0.80}(\text{PO}_4)_2$  (*b* region) shows three  ${}^5D_0 - {}^7F_0$  lines and nine  ${}^5D_0 \rightarrow {}^7F_1$  lines which confirms the isotypy with  $\text{Na}_3\text{Nd}(\text{VO}_4)_2$  (L.T.) (Fig. 5-1).

For the composition  $\text{Na}_{2.95}\text{Ca}_{0.10}\text{Eu}_{0.95}(\text{PO}_4)_2$  (*c* region), the spectrum is quite similar to that of  $\text{Na}_3\text{Eu}(\text{PO}_4)_2$  ( $\delta$  type) (Fig. 6-1).

For  $\text{Na}_{2.45}\text{Sr}_{1.10}\text{Eu}_{0.45}(\text{PO}_4)_2$  (*d* region) the emission spectrum shows the same number of lines as obtained in the *a* region. The width of these lines is, however, much larger (Fig. 4-2).

The spectrum of  $\text{Na}_{2.80}\text{Sr}_{0.40}\text{Eu}_{0.80}(\text{PO}_4)_2$  (*e* region) is also characterized by lines which are very large for a crystalline compound (Fig. 5-2).

A comparison between Fig. 2 and Fig. 6-2 shows clearly that the band observed for the  ${}^5D_0 \rightarrow {}^7F_0$  emission in the *e* region can be considered as the envelope of all possible  ${}^5D_0 \rightarrow {}^7F_0$  lines of the  $\text{Na}_3\text{Eu}(\text{PO}_4)_2$  spectrum ( $\delta + \epsilon$  types).

Tables I to V show the characteristic line positions of the  $\text{Eu}^{3+}$  emission spectra for the five regions under 380 nm excitation at  $T = 80$  K.

This band develops into a group of narrow lines as the composition comes

TABLE IV  
 ${}^5D_0 \rightarrow {}^7F_j$  ( $j = 0, 1, 2$ ) EMISSION OF  $\text{Eu}^{3+}$  IN  
 $\text{Na}_{2.45}\text{Sr}_{1.10}\text{Eu}_{0.45}(\text{PO}_4)_2$  (*d* TYPE) UNDER 380-nm  
EXCITATION ( $T = 80$  K)

<i>d</i> Type	$T = 80$ K	
	$\lambda$ (nm)	$E$ ( $\text{cm}^{-1}$ )
$\text{Na}_{2.45}\text{Sr}_{1.10}\text{Eu}_{0.45}(\text{PO}_4)_2$		
${}^5D_0 \rightarrow {}^7F_0$	579.6	17,253
	588.8	16,984
	592.5	16,878
${}^5D_0 \rightarrow {}^7F_1$	595.2	16,801
	611.4	16,356
	612.7	16,321
${}^5D_0 \rightarrow {}^7F_2$	617.4	16,197
	619.3	16,147
	622.3	16,069

TABLE V  
 ${}^5D_0 \rightarrow {}^7F_0$  EMISSION OF  $\text{Eu}^{3+}$  IN  
 $\text{Na}_{2.98}\text{Sr}_{0.04}\text{Eu}_{0.98}(\text{PO}_4)_2$  (*e* TYPE) UNDER 380-nm  
EXCITATION ( $T = 80$  K)

<i>e</i> Type	$T = 80$ K			
	$\lambda$ (nm)	$E$ ( $\text{cm}^{-1}$ )	Attribution	
$\text{Na}_{2.98}\text{Sr}_{0.04}\text{Eu}_{0.98}(\text{PO}_4)_2$	${}^5D_0 \rightarrow {}^7F_0$	578.6	17,283	$\delta$
		578.9	17,274	$\delta$
		579.0	17,271	$\delta$
		579.1	17,268	$\epsilon$
		579.5	17,256	$\epsilon$
		579.6	17,253	$\delta$
		579.7	17,250	$\delta$
		579.8	17,247	$\epsilon$
		579.9	17,244	$\delta$
		580.0	17,241	$\delta$
		580.3	17,232	$\delta$

closer to the limit  $\text{Na}_3\text{Eu}(\text{PO}_4)_2$  (Fig. 6-3). It is worthwhile to note that the widening of the emission lines, which is observed as soon as the strontium content becomes significant enough, takes place without changing the cation positions.

## Discussion

On the basis of these results one may conclude that the rare-earth ions occupy in the strontium phases a family of sites (*d* region) or several families of sites (*e* region) having an almost identical oxygen environment. The large change observed in each case in going from the calcium to the strontium phases (Fig. 6) can be explained by the increasing unit cell volume and the weakening of the  $\text{M}^{2+}-\text{O}$  bonds. Both factors facilitate the rotation of the  $[\text{PO}_4]$  group.

Such a broadening of the  $\text{Eu}^{3+}$  emission lines is normally encountered in glasses (14, 15). It may also be observed in crystalline compounds such as fast ionic conductors, e.g., stabilized yttrium-zirconia, in which the distribution of oxygen vacancies, due to the substitution of Y for Zr, is statis-

tical in the anionic sublattice. This sublattice deviates from cubic symmetry by a relaxation effect with respect to these vacancies (16).

In the phosphates the lack of definition at long range of the anionic sublattice results from the relative ability of  $[\text{PO}_4]$  tetrahedra to rotate.

In both cases, although we are dealing with crystalline compounds, the emission spectra reflect, as far as the oxygen environment is concerned, a situation similar to that observed in glasses.

### Acknowledgments

The authors thank Dr. Antic-Fidancev, Dr. Piriou, and Dr. Caro for helpful discussions, and Dr. M. Dexpert for electron diffraction investigations.

### References

1. G. GAULTIER AND G. PANNETIER, *Bull. Soc. Chim. Fr.* **1**, 105 (1968).
2. J. A. MCGINNETY, *Acta Crystallogr. Sect. B* **28**, 2845 (1972).
3. A. J. VANDEN BERG, F. TUINSTRRA, *Acta Crystallogr. Sect. B* **34**, 3177 (1978).
4. M. MIYAKE, H. MORIKAWA, AND SHIN-ICHI IWAI, *Acta Crystallogr. Sect. B* **36**, 532 (1980).
5. H. ARNOLD, W. KURTZ, A. RICHTER-ZINNIUS, J. BETHKE, AND G. HEGER, *Acta Crystallogr. Sect. B* **37**, 1643 (1981).
6. R. KLEMENT AND P. KRESSE, *Z. Anorg. Allg. Chem.* **310**, 53 (1961).
7. A. W. KOLSI, M. QUARTON, AND W. FREUNDLICH, *J. Solid State Chem.* **36**, 107 (1981).
8. M. VLASSE, C. PARENT, R. SALMON, G. LE FLEM, AND P. HAGENMULLER, *J. Solid State Chem.* **35**, 318 (1980).
9. R. SALMON, C. PARENT, M. VLASSE, AND G. LE FLEM, *Mater. Res. Bull.* **13**, 439 (1978).
10. B. PIRIOU, L. ANTIC-FIDANCEV, P. CARO, J. FAVA, C. PARENT, AND G. LE FLEM, submitted for publication.
11. M. A. BREDIG, *J. Phys. Chem.* **46**, 747 (1942).
12. M. T. PAQUES-LEDENT, *C. R. Acad. Sci. Paris* **274**, 1998 (1972).
13. C. PARENT, J. FAVA, R. SALMON, M. VLASSE, G. LE FLEM, P. HAGENMULLER, E. ANTIC-FIDANCEV, M. LEMAITRE-BLAISE, AND P. CARO, *Nouveau J. Chim.* **3**, 523 (1979).
14. R. REISFELD, *Struct. Bonding (Berlin)* **13**, 53 (1973).
15. R. REISFELD, *Struct. Bonding (Berlin)*, **22**, 123 (1975).
16. J. DEXPERT-GYS, Thèse de Doctorat-ès-Sciences, Université de Paris IX, Orsay (1979).